Mycobacterium tuberculosis suppresses protective Th17 responses during infection through multiple mechanisms

Authors: Alex Zilinskas[1], Amir Balakhmet[1], Douglas Fox[1], Heyuan Michael Ni[1], Carolina Agudelo[2], Helia Samani[1], Sarah Stanley[1,2]

Affiliations:

1. Division of Immunology and Molecular Medicine, Department of Molecular and Cell Biology, University of California, Berkeley, Berkeley, CA.
2. Division of Infectious Disease and Vaccinology, School of Public Health, University of California, Berkeley, Berkeley, CA.

Short title: M. tuberculosis subverts protective Th17s

Abstract

Mycobacterium tuberculosis (Mtb) causes more deaths annually than any other pathogen, yet an effective vaccine remains elusive. IFN-γ–producing CD4+ T cells are necessary but insufficient for immune protection. Data from humans shows that the development of IL-17a producing Th17 T cells correlates with protection against infection, however not all individuals develop a Th17 response. In mouse models, experimental vaccines can elicit protective Th17 cells, but Th17s are rare in primary infection. Here, we identify factors suppressing Th17 responses during primary Mtb infection. First, using Tbet deficient mice, we demonstrate that Mtb drives a Th1 response that is only partially protective and limits the production of protective Th17 cells in an IFN-γ independent manner. Next, we reveal that the ESX-1 type VII alternative secretion system in Mtb suppresses Th17 responses by inhibiting IL-23 production in dendritic cells. These findings define a new function of the ESX-1 secretion system in Mtb virulence, a long-standing question in tuberculosis research.

Introduction

Mycobacterium tuberculosis (Mtb), the causative agent of tuberculosis (TB), remains one of the leading infectious disease killers worldwide, with 10.6 million new cases and 1.6 million deaths reported in 2021 (World Health Organization, 2022). The current vaccine, *Mycobacterium bovis bacillus Calmette-Guérin* (BCG), protects against childhood TB, but has highly variable efficacy, wanes over time, and provides minimal protection against adult pulmonary TB (Fine, 1995; World Health Organization, 2018; Kumar, 2021). Although there are 17 vaccine candidates currently in clinical trials, achieving robust vaccine elicited immunity remains a major challenge (Zhou and Zhang, 2023).

Interferon-γ (IFN-γ) produced by type 1 T helper (Th1) cells is essential for control of Mtb infection both in animal models and in humans (Flynn et al., 1993; Condos et al., 1998; Casanova and Abel, 2002). However, the MVA85A vaccine, despite inducing robust Th1 responses as intended, failed to provide protection against Mtb infection (Ndiaye et al., 2015). Patients with active TB can have high levels of IFN-γ in the lungs despite being unable to control infection (Ledesma et al., 2011). Thus, Th1 cells are necessary but not sufficient for controlling Mtb infection suggesting that other factors are important for effective immunity. Without a comprehensive understanding of which types and specific subsets of T helper cells essential to limit Mtb infection, developing an effective Mtb vaccine with consistent high efficacy will remain elusive.

Type 17 T helper (Th17) cells are known for their association with mucosal sites, including the lungs, where they have been shown to provide protection against several bacterial and fungal respiratory pathogens (Guglani and Khader, 2010). This protection relies on IL-17a production by Th17 cells (Gaffen, 2009). Many factors determine whether Th17 cells are elicited by

65 infection. Antigen-presenting cells (APCs) drive the polarization of naïve T cells into Th17 cells
66 by producing cytokines including IL-1β, IL-6, TGF-β, and IL-23. Activation of the RORγT
67 transcription factor is essential for Th17 polarization (Lazarevic et al., 2011). There is also
68 evidence that the route of infection with a bacterial pathogen influences whether a Th17
69 response is elicited. Infection with *Listeria monocytogenes* via the intranasal, but not
70 intravenous route is required to observe a Th17 response to infection (Pepper et al., 2010).
71 Th17 differentiation is opposed by Th1 differentiation via multiple mechanisms (Huber and
72 Farrar, 2011). Tbet, the transcription factor essential for commitment to the Th1 lineage, has
73 been shown to prevent Runx1 activation, thereby preventing Runx1-mediated transactivation of
74 RORγT and therefore Th17 differentiation (Lazarevic et al., 2011). Additionally, IFN-γ, the
75 signature cytokine of Th1s, inhibits Th17 differentiation and function via activation of STAT1,
76 independent of Tbet (Yeh et al., 2014). Finally, production of type I IFN also can suppress Th17
77 differentiation (Zhang et al., 2011). Thus, several hallmarks of Mtb infection, namely strong Th1
78 responses, IFN-γ production, and type I interferon production tend to weigh against Th17s.
79 Increasing evidence that Th17 cells correlate with protection against Mtb infection both in the
80 non-human primate model (Gideon et al., 2015) and in humans (Perreau et al., 2013; Ogongo et
81 al., 2021; Nathan et al., 2021; Sun et al., 2024) suggest that Th17 cells are an important
82 component of protective immunity to Mtb. In mice, Th17 cells are rarely observed during primary
83 Mtb infection, and the conditions under which Th17 cells are induced during infection remain
84 unclear (Khader et al., 2007; Gopal et al., 2014; Segueni et al., 2016; Aguilo et al., 2016; Jong
85 et al., 2022). However, experimental TB vaccines, particularly via a mucosal route, elicit Th17
86 cells that can confer protection against subsequent challenge in mice (Khader et al., 2007; Jong
87 et al., 2022), demonstrating that Th17 cells can be protective against Mtb infection. Why Mtb
88 infection does not robustly elicit Th17 cells during primary infection, despite causing infection at
89 mucosal surfaces via airway infection, is unclear.

90 The ESX-1 type VII alternative secretion system is a fundamental determinant of Mtb virulence
91 (Stanley et al., 2003). The ESX-1 secretion system has been demonstrated to subvert and/or
92 manipulate immune responses, including by perforating phagosomal membranes, inducing
93 detrimental host type I interferon, and inducing autophagy (Stanley et al., 2007; Simeone et al.,
94 2012; Romagnoli et al., 2012). As much of the work examining ESX-1 function has been
95 conducted in vitro, we lack a clear understanding of all the factors by which ESX-1 mutants are
96 attenuated during in vivo infection. Interestingly, the Mtb lipid phthiocerol dimycocerosate
97 (PDIM) is also required for virulence and has been linked to ESX-1 function through induction of
98 type I IFN, which can suppress Th17 responses (Cox et al., 1999; Barczak et al., 2017). In
99 addition, the ESX-1 secretion system was shown to suppress production of IL-12 p40 (Stanley
100 et al., 2007), a subunit shared with IL-23, which promotes Th17 differentiation. These data
101 suggest that Mtb virulence factors, including ESX-1 and PDIM may suppress the emergence of
102 a protective Th17 response during Mtb infection.
103
104 Here we show that the induction of Th17 cells during Mtb infection is suppressed by multiple
105 mechanisms. First, we show that the absence of a Th17 response during primary infection is not
106 dependent on duration or route of infection. Instead, we show that mice lacking Tbet (*Tbx21*$^{-/-}$)
107 produce Th17 cells after Mtb infection, and that these cells provide IL-17a-dependent protection
108 to early Mtb infection. The suppression of Th17 production by Th1 cells is independent of IFN-γ.
109 Furthermore, we observe a strong Th17 response during infection with ΔESX-1 or PDIM-lacking
110 Mtb in naïve mice, suggesting that these virulence factors function to suppress Th17
111 differentiation. Surprisingly, the ability of ESX-1/PDIM to suppress Th17 differentiation is not
112 related to their enhanced induction of type I IFN. Instead, we show that during infection with
113 these strains type 2 conventional dendritic cells (CD11b^{+} DCs, cDC2s), which are known to
114 support Th17 differentiation, produce higher levels of IL-23 secretion in draining lymph nodes of
115 Mtb infected mice (Schlitzer et al., 2013). These results demonstrate that Mtb utilizes the ESX-1

secretion system and PDIM to bias host T helper response towards Th1s and away from Th17s in a manner that limits but permits Mtb infection.

Results

Th17 induction during *M. tuberculosis* infection does not depend on duration or route of infection

We first tested whether the duration or route of infection has an impact on the generation of Th17 cells during Mtb infection. To test for induction of Th17 cells, we infected wild type mice with ~100 CFU of WT *M. tuberculosis* via the aerosol route, a standard dose for the mouse model (Soldevilla et al., 2022). As previously published by multiple groups, we do not observe Th17 cells during the first month after Mtb infection of mice (Khader et al., 2007; Gopal et al., 2014; Segueni et al., 2016; Aguilo et al., 2016; Jong et al., 2022). At 4 weeks post infection, we observed the expected plateau of CFU in the lungs of infected mice indicating the onset of T cell-based control of infection (Figure 1A). With stimulation using peptide pools from model antigens ESAT-6 and Antigen 85B (Ag85B) (Andersen et al., 1995; Bekmurzayeva et al., 2013; Babaki et al., 2017), we observed only IFN-γ^+ $CD4^+$ (Th1) T cells (Figure 1B) and no IL-17a^+ $CD4^+$ (Th17) T cells at this or earlier timepoints (Figure 1C). Th17 cells have been observed in humans, at times presumably long after initial infection (Perreau et al., 2013; Ogongo et al., 2021; Nathan et al., 2021; Sun et al., 2024). We therefore tested whether Th17 cells arise at late timepoints after infection in mice. Mice continued to only have a Th1 response up to day 170 post infection (Figures 1D-E). It was previously reported that infection with the virulent HN878 “Beijing” strain of the L2 lineage resulted in induction of Th17 cells (Gopal et al., 2014). However, we did not observe a significant increase in IL-17a producing T cells in murine lungs when we infected with a Beijing strain at 3 weeks post infection (Supplementary Figure 1).

The route of bacterial infection can impact which T helper cell types are induced. Infection via the intranasal route has been shown to elicit Th17 cells in response to infection with *Listeria*

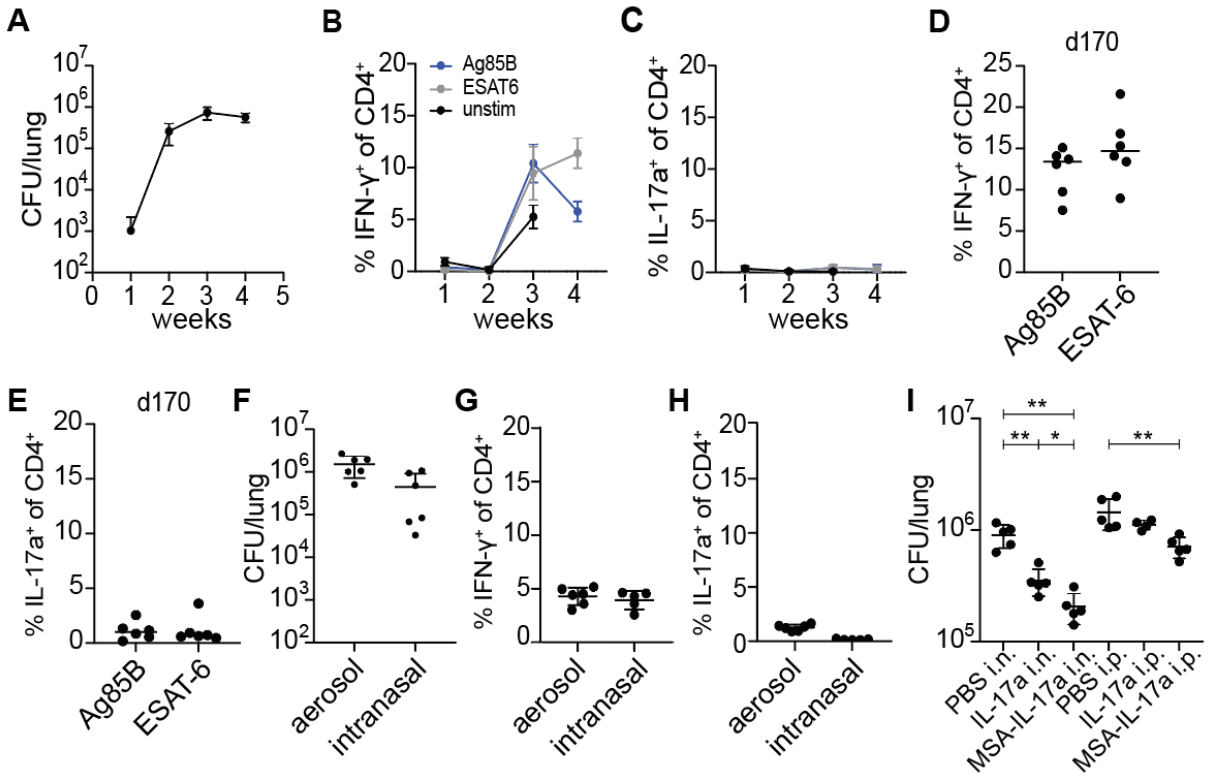

Figure 1. Lack of Th17 induction during WT *M. tuberculosis* infection is not due to duration or route of infection. (A-C) WT B6 mice were aerosol infected with WT *M. tuberculosis* Erdman strain and evaluated at 21 days post infection (dpi) for **(A)** bacterial burdens in lungs by CFU from lungs **(B)** IFN-γ$^+$ CD4$^+$ T cells and **(C)** IL-17a$^+$ CD4$^+$ T cells from lungs using flow cytometry. Cytokines were measured using ICS after restimulation with Ag85b or ESAT-6 peptide pools. **(D-E)** Mice were infected and analyzed at 170 dpi for **(D)** IFN-γ$^+$ CD4$^+$ T cells and **(E)** IL-17a$^+$ CD4$^+$ T cells in lungs using flow cytometry. **(F-H)** WT B6 mice were either aerosol infected or intranasally infected with WT *M. tuberculosis* Erdman strain and evaluated 28 dpi for **(F)** bacterial burdens in lungs by CFU, **(G)** IFN-γ$^+$ CD4$^+$ T cells and **(H)** IL-17a$^+$ CD4$^+$ T cells in lungs by flow cytometry. Cytokines were measured using ICS after restimulation with ESAT-6 peptide pool. **(I)** WT B6 mice were aerosol infected with WT *M. tuberculosis* and treated with PBS control, recombinant murine IL-17a (IL-17a) or recombinant murine IL-17a fused to murine serum albumin (MSA-IL-17a) daily either using the intranasal (i.n.) or intraperitoneal (i.p.) routes between days 11 to 20 post infection. CFU in lungs was measured at 21 dpi. Results are representative of at least 2 biological replicates. For all graphs, each dot represents an individual mouse. *$p<0.05$, **$p<0.01$ (unpaired nonparametric Mann-Whitney U test).

141 *monocytogenes* and Group A *Streptococcus* (Pepper et al., 2010; Dileepan et al., 2011). We
142 therefore tested whether the intranasal route of infection results in a Th17 response in the lungs
143 of Mtb infected mice. Mice were infected intranasally such that we inoculated ~100 CFU of WT
144 Mtb into the lungs as measured on day 1 after infection. After four weeks of infection, mice had
145 comparable levels of bacteria in the lungs between infection routes (Figure 1F). At this timepoint

146 we again observed only IFN-γ producing CD4 T cells and very few IL-17a producing CD4 T cells
147 in the lungs (Figures 1G-H). Thus, the route of infection with Mtb does not seem to impact the
148 dominant Th1-biased response observed during primary infection of naïve mice with Mtb. We
149 next investigated whether exogenous IL-17a treatment could provide protection against WT Mtb
150 infection during primary infection. WT mice aerosol infected with WT Mtb were intranasally
151 administered with either PBS control or 1 μg recombinant murine IL-17a daily between days 11
152 to 20 post infection for a total of 10 doses (Figure 1I). WT mice intranasally (i.n.) administered
153 1 μg recombinant murine IL-17a daily were slightly more protected with ~3-fold reduction in lung
154 CFU compared to WT mice given vehicle control. However, we observed no effect of IL-17a
155 when it was administered via the intraperitoneal (i.p.) route. Cytokines are known to have short
156 half-lives in vivo. Fusing a cytokine to serum albumin can increase its half-life, permitting greater
157 efficacy (Tan et al., 2022). We therefore fused IL-17a to murine serum albumin (MSA-IL-17a)
158 and administered this construct either i.p. or i.n. at equimolar quantities compared to free IL-17a
159 administered dosages. We found that i.n. delivery of this construct was more effective than
160 delivery of IL-17a, with ~5-fold decrease in CFU observed in the lungs. In addition, fusion to
161 albumin allowed us to see efficacy with i.p. administration, resulting in a ~2-fold decrease in lung
162 CFU. These results indicate that IL-17a can induce protective immunity to Mtb in the context of
163 a primary infection, and that this may have potential as a therapeutic approach.
164

165 **_Tbet_$^{-/-}$ mice are protected by a robust Th17 response during early _M. tuberculosis_**
166 **infection**

167 Because Th1 responses are known to inhibit Th17 responses (Lazarevic et al., 2011; Yeh et al.,
168 2014), we next tested whether Th1 differentiation masks a protective Th17 response during Mtb
169 infection. *Tbx21*, also referred as Tbet, encodes the essential transcription factor that drives the
170 Th1 lineage (Lazarevic et al., 2011). Interestingly, *Tbet*$^{-/-}$ mice lack Th1 T cells but are not as
171 susceptible to infection with Mtb as are *Ifng*$^{-/-}$ mice (Sullivan et al., 2005; Flynn et al., 1993). As

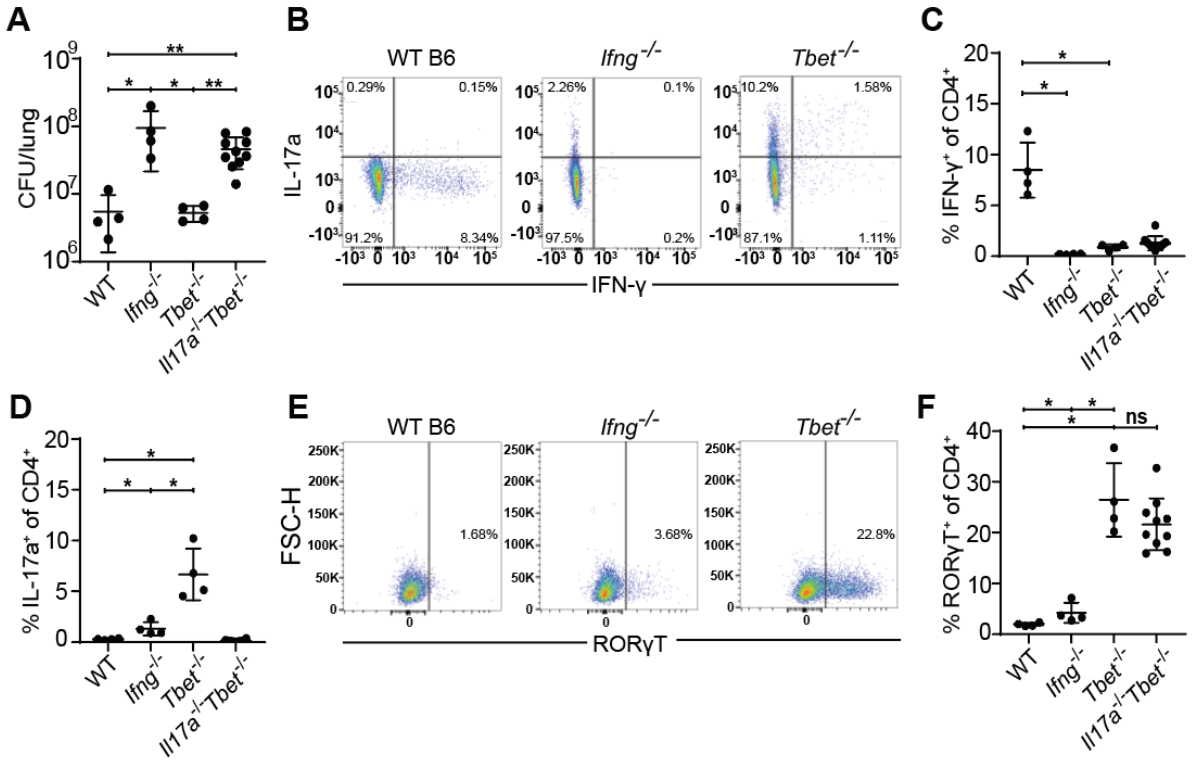

Figure 2. *Tbet*$^{-/-}$ mice are protected from susceptibility to Mtb infection by the emergence of Th17 cells. WT B6, *Ifng*$^{-/-}$, *Tbet*$^{-/-}$, and *Tbet*$^{-/-}$*Il17a*$^{-/-}$ mice were aerosol infected with WT *M. tuberculosis* Erdman strain. *Tbet*$^{-/-}$ and *Tbet*$^{-/-}$*Il17a*$^{-/-}$ mice were littermate-controlled. Mice were infected with Mtb and evaluated 21 days post infection for **(A)** CFU in the lungs of indicated genotypes or **(B-F)** cellular immune responses during flow cytometry. CD4$^+$ T cells were gated on single, live, MHC-II$^-$, Ly6G$^-$, CD3$^+$, γδTCR$^-$, CD4$^+$, CD8a$^-$ cells for analysis of IFN-γ **(B,C)**, IL-17 **(B,D)** and RORγT **(E,F)**. Results in B-E are representative of 3 independent experiments. *, $p < 0.05$; **, $p < 0.01$ (unpaired nonparametric Mann-Whitney U test).

expected, we found that *Ifng*$^{-/-}$ mice were extremely susceptible to infection with Mtb, however *Tbet*$^{-/-}$ had CFU in the lungs equivalent to wild type mice at 21 days after infection (Figure 2A). Only WT mice had IFN-γ producing CD4 T cells in the lungs at this timepoint (Figures 2B, 2C). Importantly, *Tbet*$^{-/-}$ mice exhibited a robust population of IL-17a producing CD4 T cells at 3 weeks post infection, confirming that Tbet prevents Th17 differentiation during Mtb infection (Figures 2B, 2D). Importantly, IFN-γ deficient mice did not exhibit elevated levels of IL-17a producing CD4 T cells demonstrating that IFN-γ production is not the mechanism by which Th1 T cells limit a Th17 response during Mtb infection (Figure 2D).

180 A previous study demonstrated that Tbet constrains effective T cell responses by promoting the
181 differentiation of terminally differentiated, non-protective intravascular Th1 T cells (Sallin et al.,
182 2017). This study also used antibody blockade of IL-17a in Tbet deficient mice to conclude that
183 IL-17a provides minimal protection in this setting (Sallin et al., 2017). However, given that
184 antibody blockade is limited by its short duration and possibly incomplete inhibition, we tested
185 whether genetically ablating IL-17a production in Tbet mice enhanced their susceptibility to Mtb
186 infection. We therefore infected *Tbet*$^{-/-}$ and *Tbet*$^{-/-}$*Il17a*$^{-/-}$ (*Il17a*$^{icre/icre}$ referred to as *Il17a*$^{-/-}$)
187 littermate-controlled mice with Mtb and measured CFU and T cell responses in the lungs after 3
188 weeks of infection. *Tbet*$^{-/-}$*Il17a*$^{-/-}$ mice were highly susceptible to Mtb infection with a 10-fold
189 increase in lung CFU compared to WT and *Tbet*$^{-/-}$ mice, similar to the susceptibility observed in
190 *Ifng*$^{-/-}$ mice (Figure 2A). *Tbet*$^{-/-}$*Il17a*$^{-/-}$ mice completely lacked both IFN-γ producing (Figure
191 2C) and IL-17a producing CD4 T cells (Figure 2D). Notably, *Tbet*$^{-/-}$*Il17a*$^{-/-}$ mice still generated
192 Th17 cells, as evidenced by the presence of the Th17 master transcription factor RORγT
193 (Lazarevic et al., 2011), despite their inability to produce IL-17a (Figures 2E, 2F). Together,
194 these results indicate that IL-17a production by Th17 cells confers significant protection
195 against Mtb infection in *Tbet*$^{-/-}$ mice, at least during early stages of infection.
196

197 ***M. tuberculosis* utilizes ESX-1 and PDIM to limit Th17 response in mice**

198 We next examined whether Mtb utilizes virulence factors to alter the host T helper response.
199 The ESX-1 secretion system and the complex lipid PDIM are both known to influence
200 production of cytokines known to impact Th17 differentiation (Stanley et al., 2007; Barczak et
201 al., 2017; Hinman et al., 2021). Furthermore, these systems have been proposed to operate in
202 the same virulence promoting pathway (Barczak et al., 2017; Augenstreich et al., 2017). We
203 therefore tested whether ESX-1 and PDIM might promote virulence in part by suppressing Th17
204 differentiation (Figure 3A). To test for a role of the ESX-1 secretion system, we infected mice

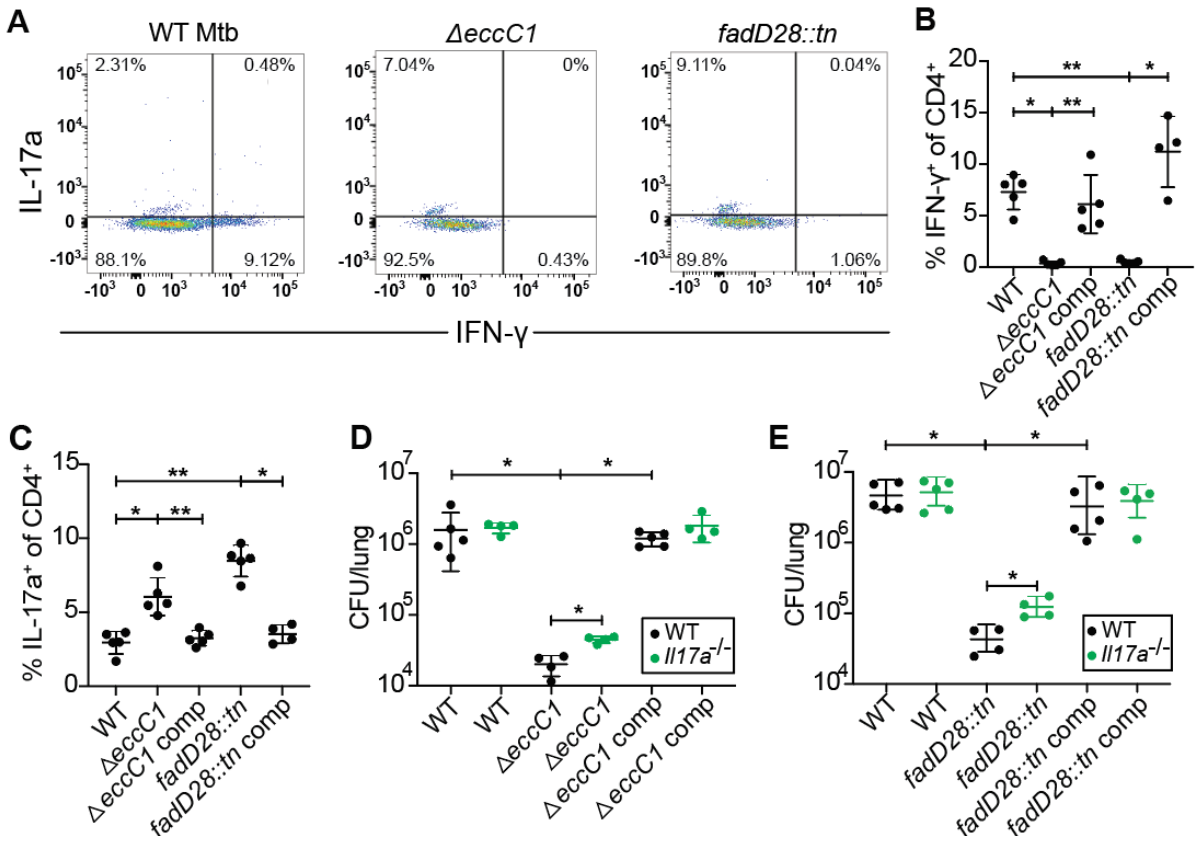

Figure 3. *M. tuberculosis* ESX-1 and PDIM virulence factors suppress Th17 response in mice. WT B6 mice were aerosol infected with indicated strains and evaluated at 21 days post infection. **(A)** Representative flow cytometry plots (cells gated on single, live, MHC-II$^-$, Ly6G$^-$, CD3$^+$, γδTCR$^-$, CD4$^+$, CD8a$^-$) of IFN-γ$^+$ and IL-17a$^+$ CD4$^+$ T cell populations. 21 days post infection, mice were sacrificed and evaluated ESAT-6 peptide pool stimulated lung homogenates for **(B)** IFN-γ$^+$ CD4$^+$ T cells and **(C)** IL-17a$^+$ CD4$^+$ T cells by flow cytometry. **(E)** Littermate-controlled WT B6 and *Il17a*$^{-/-}$ mice were aerosol infected with indicated strains at 21 days post infection with lung homogenate plated for CFU. Results are representative of 2 independent experiments. *, $p < 0.05$; **, $p < 0.01$ (unpaired nonparametric Mann-Whitney U test).

with Δ*eccC1,* which lacks an ATPase required for ESX-1 function (ΔESX-1) (Crosskey et al., 2020) (Supplementary Figure 2). We also utilized a mutant with an inactivating transposon insertion in *fadD28*, a gene required for PDIM biosynthesis (*fadD28::tn*, PDIM-lacking) (Cox et al., 1999) (Supplementary Figure 2). As expected, ΔESX-1 and PDIM-lacking mutants were highly attenuated during infection at 3 weeks, exhibiting a 100-fold reduction in bacterial burden while complemented strains had similar CFU as WT Mtb (Supplementary Figure 3). Interestingly, ESAT-6 peptide pool stimulation of lung cells in ΔESX-1 and PDIM-lacking Mtb

212 infected mice had an ~5-fold reduction in %IFN-γ$^+$ of CD4$^+$ T cells (Th1s) (Figure 3B) and ~2-
213 fold increase in %IL-17a$^+$ of CD4$^+$ T cells (Th17s) (Figure 3C) compared to complements of
214 either mutant or WT Mtb. Similar results were seen with Ag85b peptide pool stimulation
215 (Supplementary Figure 4). We tested if the induced Th17s are providing protection mediated by
216 IL-17a by infecting littermate-controlled WT B6 and *Il17a*$^{-/-}$ mice with either WT, ΔESX-1, or
217 complemented ΔESX-1 Mtb, or either WT, PDIM-lacking, or complemented PDIM-lacking Mtb.
218 Under the conditions where Th17s are highly induced, mice infected with either ΔESX-1 or
219 PDIM-lacking Mtb, the *Il17a*$^{-/-}$ mice had ~3-5 fold higher CFU than WT mice (Figures 3D, 3E).
220 These results indicate that Mtb utilizes ESX-1 and PDIM to prevent the induction of a Th17
221 response that enhances protection against Mtb infection.
222
223 **Type I interferons boost Th1 induction and do not impact Th17 induction**
224 As ESX-1 and PDIM are responsible for the host type I interferon response to Mtb infection
225 (Stanley et al., 2007; Barczak et al., 2017), and type I IFN is known to suppress Th17 responses
226 (Zhang et al., 2011), we investigated the impact of type I interferon signaling on Th17 induction
227 during Mtb infection. We examined the effect of type I IFN both in WT B6 mice, and in *Sp140*$^{-/-}$
228 mice that are highly susceptible to infection because of an excessive type I IFN response to
229 infection (Ji et al., 2019). To abrogate type I IFN in each background we used mice deficient for
230 the type I IFN receptor IFNAR. WT, *Ifnar1*$^{-/-}$, *Sp140*$^{-/-}$, *Sp140*$^{-/-}$*Ifnar1*$^{-/-}$, *Ifng*$^{-/-}$, and *Tbet*$^{-/-}$ mice
231 were aerosol infected with WT Mtb. As expected, both *Sp140*$^{-/-}$ and *Ifng*$^{-/-}$ mice had up to 10-
232 fold higher CFU than WT mice while *Ifnar1*$^{-/-}$, *Sp140*$^{-/-}$*Ifnar1*$^{-/-}$, and *Tbet*$^{-/-}$ mice were as
233 resistant as WT mice at 3 weeks post infection (Figure 4A). *Sp140*$^{-/-}$ mice had an almost 2-fold
234 increase in %IFN-γ$^+$ of CD4$^+$ (Th1) T cells compared to WT mice, *Ifnar1*$^{-/-}$ had a 2-fold reduction
235 in %IFN-γ$^+$ of CD4$^+$ (Th1) T cells compared to WT mice, *Sp140*$^{-/-}$*Ifnar1*$^{-/-}$ mice had a slightly
236 stronger 4-fold reduction in %IFN-γ$^+$ of CD4$^+$ (Th1) T cells compared to *Sp140*$^{-/-}$ mice (Figures
237 4B-D). Importantly, deletion of IFNAR had no impact on Th17 induction in either WT or *Sp140*$^{-/-}$

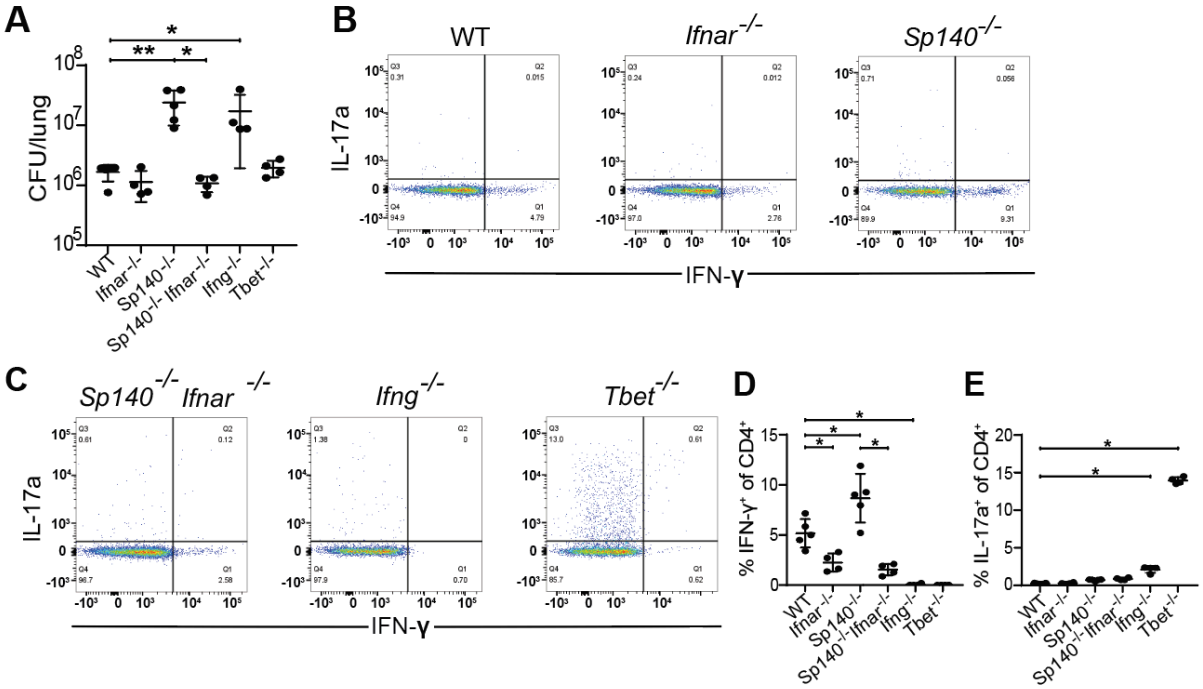

Figure 4. Type I interferon signaling boosts Th1 induction and does not impact Th17 induction. WT B6, *Ifnar*$^{-/-}$, *Sp140*$^{-/-}$, *Sp140*$^{-/-}$*Ifnar*$^{-/-}$, *Ifng*$^{-/-}$, and *Tbet*$^{-/-}$ mice were aerosol infected with WT *M. tuberculosis* Erdman strain. **(B, C)** Representative flow cytometry plots (cells gated on single, live, MHC-II^{-}, Ly6G^{-}, CD3^{+}, γδTCR^{-}, CD4^{+}, CD8a^{-}) of IFN-γ^{+} and IL-17a^{+} CD4^{+} T cells of these populations. 21 days post infection, lung homogenates were measured for **(A)** CFU and analyzed via flow cytometry for **(D)** IFN-γ^{+} CD4^{+} T cells and **(E)** IL-17a^{+} CD4^{+} T cells. Results in A, D, and E are representative of 2 independent experiments. *, $p < 0.05$; **, $p < 0.01$ (unpaired nonparametric Mann-Whitney U test).

mice, although we observed the expected increase in Th17 cells in Tbet deficient animals (Figure 4E). These results indicate that type I interferon signaling only impacts the induction of Th1s with positive correlation while type I interferon signaling does not influence Th17 induction, suggesting that induction of type I IFN by ESX-1/PDIM is not the mechanism by which these virulence factors suppress Th17 differentiation.

ESX-1 and PDIM alter conventional dendritic cell cytokine signaling in the mediastinal lymph node

Previous work suggested that ESX-1 mutants fail to suppress IL-12 p40, a subunit shared between IL-12 and IL-23, expression from infected macrophages in vitro (Stanley et al., 2007).

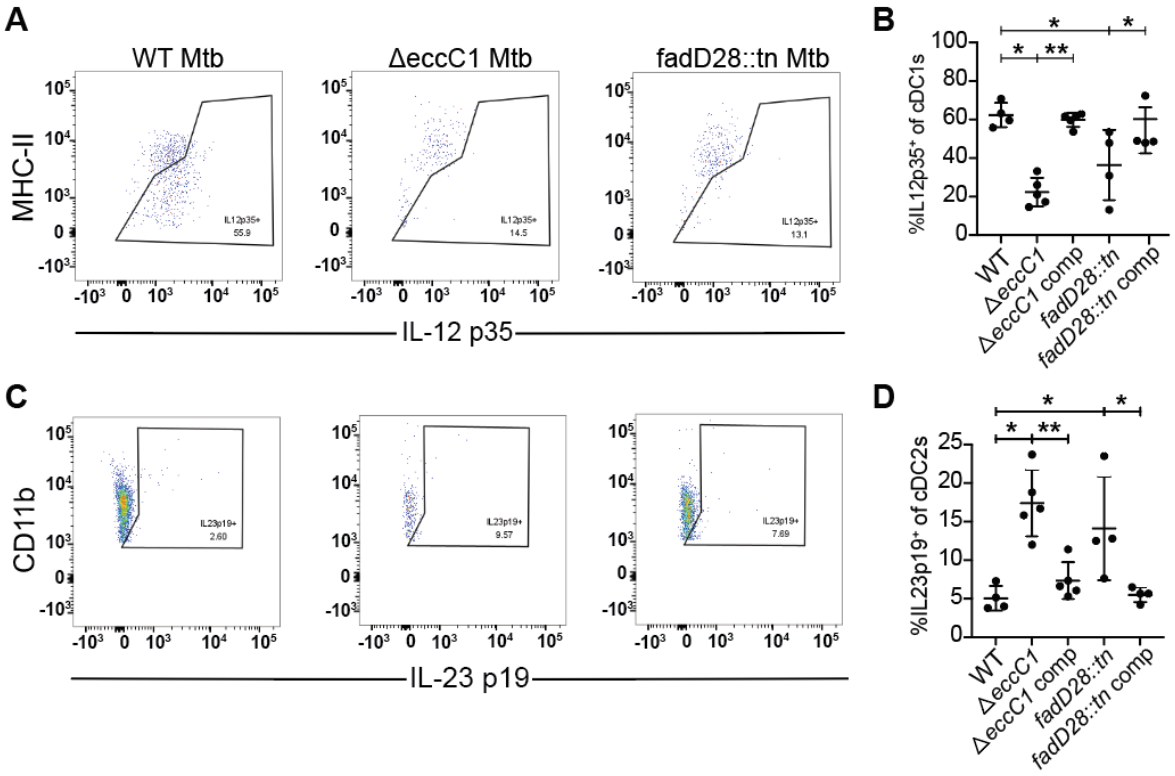

Figure 5. ESX-1 and PDIM alter conventional dendritic cell cytokine signaling in the mediastinal lymph node. WT B6 mice were aerosol infected with indicated strains and analyzed at 21 days post infection **(A,C)** Flow cytometry schematic for gating of **(A)** cDC1 (gated on single, live, $CD3^-$, $CD19^-$, $CD11c^+$, MHC-II^+, $XCR1^+$, $CD11b^-$) and **(B)** cDC2 (gated on single, live, $CD3^-$, $CD19^-$, $CD11c^+$, MHC-II^+, $XCR1^-$, $CD11b^+$) populations of mediastinal lymph nodes with representative flow cytometry plots of IL-12 $p35^+$ and IL-23 $p19^+$ gating of cDC1 and cDC2 populations respectively. 21 days post infection, mediastinal lymph nodes from WT B6 mice were aerosol infected with either WT, ΔeccC1 (ΔESX-1), complemented ΔeccC1::eccC1, transposon-inserted fadD28::tn (PDIM-lacking),or complemented transposon-inserted fadD28::tn + pfadD28 *M. tuberculosis* Erdman strain were extracted and analyzed for IL-12 $p35^+$ cDC1s **(C)** and IL-23 $p19^+$ cDC2s **(D)** by flow cytometry. Results in B and D are representative of 2 independent experiments. *, $p < 0.05$; **, $p < 0.01$ (unpaired nonparametric Mann-Whitney U test).

Because IL-23 promotes Th17 responses, and ESX-1 and PDIM are responsible for the lack of a Th17 response during Mtb infection, we next investigated if ESX-1 and PDIM suppress IL-23 production by dendritic cells during in vivo infection. We infected mice with ~100 CFU via the aerosol route and harvested mediastinal lymph nodes at 21 days post infection. We examined IL-12 and IL-23 production by conventional dendritic cells using ICS. To clearly distinguish between levels of these two cytokines we used ICS for the cytokine specific subunits: IL-12 p35

254 and IL-23 p19. First, we found that type 1 conventional dendritic cells (cDC1s), known to be
255 specialized for IL-12 production, produce robust levels of IL-12 p35 during infection with WT Mtb
256 (Figures 5A, 5B). However, both ESX-1 and PDIM deficient strains elicited significantly lower
257 levels of IL-12 p35 from these cells (Figures 5A, 5B), consistent with the lower bacterial burdens
258 in the lungs of mice infected with these mutants (Supplementary Figure 3). During infection with
259 wild-type bacteria, we observed very little IL-23 p19 production by type 2 conventional dendritic
260 cells (cDC2s) in the draining mediastinal lymph node (Figures 5C, 5D). Importantly, ESX-1 and
261 PDIM-lacking Mtb infection resulted in a dramatic increase in the percentage of cDC2s that
262 produce IL-23 p19 in mediastinal LNs (Figures 5C, 5D). We saw very little to no IL-23 p19
263 expression in cDC1s and IL-12 p35 expression in cDC2s with no differences between WT or
264 ESX-1 and PDIM deficient strains (Supplementary Figure 5). These results indicate that the
265 ESX-1 and PDIM virulence factors impact naïve T cell differentiation at the draining mediastinal
266 lymph node by promoting IL-12, a Th1-polarizing cytokine, and limiting IL-23, a Th17-polarizing
267 cytokine, expression in cDC1s and cDC2s respectively.

268 Discussion

269 Immunity against *M. tuberculosis* (Mtb) requires T helper cell responses and IFN-γ as
270 demonstrated by susceptibility of *Rag1*$^{-/-}$ (Lai et al., 2024) and *Ifng*$^{-/-}$ (Flynn et al., 1993) mice,
271 and high co-morbidity between tuberculosis and low CD4 T helper cell counts in humans with
272 AIDS (Amelio et al., 2019; Geremew et al., 2020). The requirement of a highly efficacious Mtb
273 vaccine that elicits a T helper response strong enough to provide protection against Mtb
274 infection remains desired. The MVA85A vaccine candidate elicited a strong Th1 response yet
275 failed to provide protection against Mtb infection (Ndiaye et al., 2015) illustrating that a strong
276 Th1 response is not enough to control Mtb infection. The development of a highly efficacious
277 Mtb vaccine requires a rigorous understanding of which T helper cell types and subsets provide
278 protection against Mtb infection. The recent reports of Th17s correlating to protection against

279 Mtb infection in non-human primates (Gideon et al., 2015) and humans (Perreau et al., 2013;
280 Ogongo et al., 2021; Nathan et al., 2021; Sun et al., 2024) suggest a protective role for Th17s in
281 controlling Mtb infection. Herein, we showed that Th17s can provide protection that is IL-17a-
282 dependent in mice, Mtb's ESX-1 secretion system and PDIM enhance infection at least in part
283 by preventing a Th17 response in mice, and exogenous IL-17a is protective against Mtb
284 infection.
285
286 We have previously reported that infection in unvaccinated mice does not elicit a Th17
287 response, only a Th1 response, and that an intranasally administered cyclic dinucleotide
288 adjuvant Mtb protein subunit vaccine elicits enhanced protection to Mtb infection in mice
289 mediated by Th17s and in-particular IL-17a (Van Dis et al., 2018; Jong et al., 2022). There have
290 been conflicting reports about Th17s and in-particular IL-17a providing protection against Mtb
291 infection in the murine model of tuberculosis (Khader et al., 2007; Gopal et al., 2014; Segueni et
292 al., 2016; Aguilo et al., 2016; Jong et al., 2022). Here, we report that Mtb prevents induction of
293 Th17s during primary infection via the virulence factors ESX-1 and PDIM. Others have shown
294 that intranasal vaccination of BCG, which lacks a functional ESX-1, also induced Th17s that
295 provide protection against Mtb infection (Aguilo et al., 2016).
296
297 ESX-1 and PDIM have both been shown to be required for the permeabilization of *M.*
298 *tuberculosis*-containing phagosomes and therefore induce the type I interferon response
299 (Barczak et al., 2017; Stanley et al., 2007; Augenstreich et al., 2017; Watson et al., 2015). Thus,
300 we investigated how impactful the type I interferon response is on the induction of Th1s and
301 Th17s during WT *M. tuberculosis* infection. We found that the type I interferon response boosts
302 the magnitude of the Th1 response but does not impact the induction of Th17s during *M.*
303 *tuberculosis* infection. Additionally, we show that ESX-1 and PDIM promote IL-12 and limit IL-23
304 expression in conventional dendritic cells in the draining mediastinal lymph node during *M.*

305 *tuberculosis* infection. Future work will focus on which immune pathways impacted by ESX-1
306 and PDIM gate-keep the induction of Th1 vs Th17 responses.
307
308 One possible answer for why humans induce Th1s and Th17s to Mtb infection while mice only
309 induce Th1s might be because humans evolved cDC2s capable of expressing Th1-polarizing
310 cytokine IL-12 and Th17-polarizing cytokines IL-1β, IL-6, and IL-23 (Rojas et al., 2017), and
311 mice have evolved cDC2s incapable of IL-12 expression but still capable of expressing Th17-
312 polarizing cytokines (Schlitzer et al., 2013).
313
314 A method of reliably inducing Th17s in mice during wild-type Mtb infection needs to be
315 established to effectively study the role of Th17-mediated protection. Mice lacking Tbet (as
316 known as *Tbx21*) respond to WT Mtb infection with a Th17 response and provide protection
317 mediated by IL-17a during early infection. *Tbet*$^{-/-}$ mice can be used as a model to effectively
318 study how Th17s can provide protection against early Mtb infection in the absence of Th1s. We
319 show that exogenous IL-17a treatment promotes control of Mtb infection indicating that there
320 are some cells capable of sensing IL-17a and responding in a beneficial way for the host. The
321 mechanisms by which IL-17a signaling promotes clearance of Mtb remains unknown. High Th17
322 plasticity permits Th17s to express a wide variety of T helper subset profiles and can range from
323 pro-inflammatory Th17.1s that co-express IFN-γ and IL-17a to anti-inflammatory Tr1-like Th17s
324 that co-express IL-10 and IL-17a (Stadhouders et al., 2018). Moving forward, it will be important
325 to delineate in depth which Th17 subsets and which mechanisms downstream of IL-17 receptor
326 signaling are important for controlling Mtb infection.
327
328 We have shown that Mtb utilizes the ESX-1 secretion system and lipid virulence factor PDIM to
329 prevent Th17 induction during infection. Furthermore, ESX-1 and PDIM promotes expression of
330 Th1-polarizing cytokine IL-12 in cDC1s and limits expression of Th17-polarizing cytokine IL-23

331 in cDC2s in the draining mediastinal lymph node. The type I interferon response induced by
332 ESX-1 and PDIM only boosts Th1 induction and does not impact Th17 induction. Additionally,
333 we have developed a model of inducing Th17s in mice (*Tbet*$^{-/-}$ mice) during early Mtb infection
334 which provide protection via IL-17a. And lastly, exogenous IL-17a treatment provides protection
335 against Mtb infection. With this information, our understanding of how Mtb alters the host
336 immune response to limit control of infection, and our development of models for studying Th17-
337 mediated protection against Mtb infection provide insights to guide future Mtb vaccine design
338 strategies.
339
340

341 # Materials and Methods

342 **Ethics statement**

343 All procedures involved with the use of mice were approved by the University of California,
344 Berkeley's Institutional Animal Care and Use Committee (protocol 2015-09-7979). All protocols
345 conform to federal regulations, the National Research Council Guide for the Care and Use of
346 Laboratory Animals, and the Public Health Service Policy on Humane Care and Use of
347 Laboratory Animals.

348 **Bacterial Culture**

349 *Mycobacterium tuberculosis* strain Erdman was grown in Middlebrook 7H9 liquid medium
350 supplemented with 10% oleic acid, albumin, dextrose, and catalase (OADC) (BD 212351), 0.4%
351 glycerol, and 0.05% Tween 80 or on solid 7H10 agar plates supplemented with 10% OADC and
352 0.4% glycerol. Frozen stocks of *M. tuberculosis* were made from a single culture and used for all
353 experiments.

354 **Mice**

355 C57BL/6J (no. 000664), *Ifng*$^{-/-}$ (B6.129S7-*Ifng*^{tm1Ts}/J, no. 002287), *Tbet*$^{-/-}$ (*Tbx21*$^{-/-}$, B6.129S6-
356 *Tbx21*^{tm1Glm}/J, no. 004648), and *Il17a*$^{icre/icre}$ (*Il17a*$^{-/-}$, B6.129(SJL)-*Il17a*$^{tm1.1(icre)Stck}$/J, no. 035717)
357 mice were obtained from The Jackson Laboratory and bred in-house. *Ifnar1*$^{-/-}$, *Sp140*$^{-/-}$, and
358 *Sp140*$^{-/-}$*Ifnar1*$^{-/-}$ mice were obtained from the Vance laboratory (UC Berkeley) and bred in-
359 house. Mice were age matched for all experiments.

360 **Aerosol challenge experiments with *M. tuberculosis***

361 Mice between the age of 8 to 12 weeks old were infected via the aerosol route with *M.*
362 *tuberculosis* strain Erdman using a nebulizer and full-body inhalation exposure system (Glas-
363 Col, Terre Haute, IN). A total of 9 mL of diluted aerosol stock in MiiliQ water was loaded into the
364 nebulizer to deliver 30-100 bacteria per mouse as measured by whole lung CFU 1 day post
365 infection.

366 **Intranasal challenge experiments with *M. tuberculosis***

367 Mice between the age of 8 to 12 weeks old were infected with 40 uL of *M. tuberculosis* strain
368 Erdman diluted in PBS administration for mice to inhale 30-100 bacteria per mouse as
369 measured by whole lung CFU 1 day post infection.

370 **Flow Cytometry**

371 Whole lungs were homogenized using GentleMACS C tubes (Miltenyi Biotec 130-093-237) in
372 complete RPMI-1640 media supplemented with 10% FBS, 1 mM sodium pyruvate (Sigma
373 Aldrich S8636), 0.01 mM HEPES, 1% Glutamax (Thermo Scientific 35050061), 1% non-
374 essential amino acids (Gibco 11140-050), and 55 μM 2-mercaptoethanol (Gibco 21985-023)
375 containing Liberase TM (Sigma Aldrich 05401119001) and DNase I (Sigma Aldrich
376 11284932001). Cells were stained with live/dead stain (ThermoFisher L23101), Fc block
377 (Biolegend 101320), and surface stained with antibodies for CD3, Ly6G, CD4 (BD 740268,
378 551460, and 569182 respectively), MHC-II, pan-γδTCR, and CD8a (Biolegend 107605, 118124,
379 and 100714 respectively) in Brilliant stain buffer (BD 566349). Cells were fixed and
380 permeabilized with Foxp3 staining kit (Invitrogen 00-5523-00) before intracellular staining for
381 RORγT, Foxp3 (BD 564723 and 562996 respectively), Tbet, IFN-γ, and IL-17a (Biolegend
382 644817, 505814, and 506903 respectively). Data were collected using a BD Symphony A3 flow
383 cytometer (BD) and analyzed using FlowJo Software (BD).

384 Mediastinal lymph nodes were homogenized using complete RPMI-1640 containing Liberase
385 TM (Sigma Aldrich 05401119001) and DNase I (Sigma Aldrich 11284932001) with sterile
386 plunger of 3 mL syringe to pass dissociated tissue through 100 micron cell strainer. Cells were
387 stained with live/dead stain (ThermoFisher L34966), Fc block (Biolegend 101320) and surface
388 stained with antibodies for XCR1, CD11b, CD11c, Ly6G, MHC-II, CD3, CD19 (Biolegend
389 148220, 101261, 117318, 127627, 107606, 100233, and 115545 respectively) and Ly6C and
390 CD64 (BD 755198 and 569507 respectively) in Brillant stain buffer (BD 566349). Cells were
391 fixed and permeabilized with Foxp3 staining kit (Invitrogen 00-5523-00) before intracellular

staining for IL-12 p35 (Invitrogen MA5-23559) and IL-23 p19 (BD 565317). Data were collected using a BD Symphony A3 flow cytometer (BD) and analyzed using FlowJo Software (BD).

Exogeneous IL-17a administration

Mice were intranasally administered 1 µg endotoxin-free recombinant murine IL-17a (R&D systems, 7956-ML-100/CF) in 40 µL sterile PBS daily or 40 µL of vehicle control daily, or intraperitoneally administered 2 µg endotoxin-free recombinant murine IL-17a in 100 µL sterile PBS daily or 100 uL of vehicle control dailiy from days 11 to 20 post aerosol *M. tuberculosis* challenge.

MSA-IL-17a was generated by fusing a (GGGGS)3 linker between the C-terminus of mature murine serum albumin and N-terminus of mature murine IL-17a. MSA-IL-17a was purchased from Genscript USA, Inc. in endotoxin-free pH 7.2 PBS. Mice were intranasally administered 5.54 µg MSA-IL-17a (equimolar to 1 µg recombinant murine IL-17a) in 40 µL sterile PBS daily or 40 µL vehicle control, or intraperitoneally administered 11.09 µg MSA-IL-17a (equimolar to 2 µg recombinant murine IL-17a) in 100 µL PBS or 100 µL vehicle control daily between days 11 to 20 post aerosol *M. tuberculosis* challenge.

Statistical Analysis

All data was analyzed using FlowJo v10 (FlowJo, LCC) and/or Prism 10 (GraphPad Software). All graphs were analyzed using Mann-Whitney U-test. Significant values are symbolized with asterisks of * < 0.05, ** < 0.01, and ns for non-significant.

412 # Acknowledgements

413 We thank Russell Vance's lab for the kind gifts of *Sp140*$^{-/-}$, *Ifnar1*$^{-/-}$, and *Sp140*$^{-/-}$*Ifnar1*$^{-/-}$ mice.
414 We thank Jeff Cox's lab for the kind gifts of ΔESX-1 (ΔeccC1), complemented ΔESX-1, PDIM-
415 lacking (fadD28::tn), and complemented PDIM-lacking Erdman strains. We thank Helia Samani,
416 Scott Espich, Vicky Wu, Malia Wilson, and Cielo Kwon for assistance in mouse colony
417 maintenance. We thank members of the Stanley, Cox, and Vance laboratories for helpful
418 discussions. SAS is a member of the Scientific Advisory Board for Xbiotix Therapeutics. This
419 work was funded by NIH P01 AI063302 to S.A.S.

References

1. Geneva: World Health Organization. 2022. Global Tuberculosis Report 2022. https://www.who.int/publications/i/item/9789240061729 (accessed October 5, 2024).
2. Fine, P. E. M. 1995. Variation in protection by BCG: implications of and for heterologous immunity. *The Lancet* 346(8986):1339-1345. doi:10.1016/S0140-6736(95)92348-9.
3. Geneva: World Health Organization. 2018. Global Tuberculosis Report 2018. https://apps.who.int/iris/bitstream/handle/10665/274453/9789241565646-end.pdf?sequence=1&isAllowed=y (accessed October 5, 2024).
4. Kumar, P. 2021. A Perspective on the Success and Failure of BCG. *Front Immunol* 12:778028. doi:10.3389/fimmu.2021.778028.
5. Zhou, F., and D. Zhang. 2023. Recent advance in the development of tuberculosis vaccines in clinical trials and virus-like particle-based vaccine candidates. *Front Immunol* 14:1238649. doi: 10.3389/fimmu.2023.1238649.
6. Flynn, J. L., J. Chan, K. J. Triebold, D. K. Dalton, T. A. Stewart, and B. R. Bloom. 1993. An essential role for interferon gamma in resistance to *Mycobacterium tuberculosis* Infection. *J Exp Med* 178(6):2249-2254. doi: 10.1084/jem.178.6.2249.
7. Condos, R., W. N. Rom, Y. M. Liu, and N. W. Schluger. 1998. Local Immune Response Correlate with Presentation and Outcome in Tuberculosis. *Am J Respir Crit Care Med* 157:729-735. doi: 10.1164/ajrccm.157.3.9705044.
8. Casanova, J. and L. Abel. 2002. Genetic Dissection of Immunity to Mycobacteria: The Human Model. *Annu Rev Immunol* 20:581-620. doi: 10.1146/annurev.immunol.20.081501.125851.
9. Ndiaye, B. P., D. Thienemann, M. Ota, B. S. Landry, M. Camara, S. Dièye, T. N. Dieye, H. Esmail, R. Goliath, K. Huygen, V. January, I. Ndiaye, T. Oni, M. Raine, M. Romano, I. Satti, S. Shutton, A. Thiam, K. A. Wilkinson, S. Mboup, R. J. Wilkinson, and H. McShane.

445 2015. Safety, immunogenicity, and efficacy of the candidate tuberculosis vaccine
446 MVA85A in healthy adults infected with HIV-1: a randomized, placebo-controlled, phase
447 2 trial. *Lancet Respir Med* 3(3):190-200. doi: 10.1016/S2213-2600(15)00037-5.
448 10. Ledesma, J. R., J. Ma, P. Zheng, J. M. Ross, T. Vos, and H. H. Kyu. 2021. Interferon-
449 gamma release assay levels and risk of progression to active tuberculosis: a systematic
450 review and dose-response meta-regression analysis. *BMC Infect Dis* 21(1):467. doi:
451 10.1186/s12879-021-06141-4.
452 11. Guglani, L. and S. A. Khader. 2010. Th17 cytokines in mucosal immunity and
453 inflammation. Curr Opin HIV AIDS 5(2):120-127. doi: 10.1097/COH.0b013r328335c2f6.
454 12. Gaffen, S. L. 2009. Structure and signalling in the IL-17 receptor family. *Nat Rev*
455 *Immunol* 9(8):556-567. doi: 10.1038/nri2586.
456 13. Lazarevic, V., X. Chen, J. Shim, E. Hwang, E. Jang, A. N. Bolm, M. Oukka, V. K.
457 Kuchroo, and L. H. Glimcher. 2011. Transcription factor T-bet represses T_H17
458 differentiation by preventing Runx1-mediated activation of the RORγT gene. *Nat*
459 *Immunol* 12(1):96-104. doi: 10.1038/ni.1969.
460 14. Pepper, M., J. L. Linehan, A. J. Pagán, T. Zell, T. Dileepan, P. P. Cleary, and M. K.
461 Jenkins. 2010. Different routes of bacterial infection induced long-lived T_H1 memory cells
462 and short-lived T_H17 cells. *Nat Immunol* 11:83-89. doi: 10.1038/ni.1826.
463 15. Huber, J. P., and J. D. Farrar. 2011. Regulation of effector and memory T-cell functions
464 by type I interferon. *Immunology* 132(4):466-474. doi: 10.1111/j.1365-
465 2567.2011.03412.x.
466 16. Yeh, W., I. L. McWilliams, and L. E. Harrington. 2014. IFNγ inhibits Th17 differentiation
467 and function via Tbet-dependent and Tbet-independent mechanisms. *J Neuroimmunol*
468 267(0):20-27. doi: 10.1016/j.jneuroim.2013.12.001.

469 17. Zhang, L., Yuan, S., Cheng, G., and B. Guo. 2011. Type I IFN Promotes IL-10
470 Production from T cells to Suppress Th17 Cells and Th17-Associated Autoimmune
471 Inflammation. *PLoS One* 6(12):e28432. doi: 10.1471/journal.pone.0028432.
472 18. Gideon, H. P., J. Phuah, A. J. Myers, B. D. Bryson, M. A. Rodgers, M. T. Coleman, P.
473 Maiello, T. Rutledge, S. Marino, S. M. Fortune, D. E. Kirschner, P. L. Lin, and J. L. Flynn.
474 2015. Variability in Tuberculosis Granuloma T Cell Responses Exists, but a Balance of
475 Pro- and Anti-inflammatory Cytokines Is Associated with Sterilization. *PLoS Pathog*
476 11(1):e1004603. doi: 10.1371/journal.ppat.1004603.
477 19. Perreau, M., V. Rozot, H. C. Welles, F. Belluti-Enders, S. Vigano, M. Maillard, G. Dorta,
478 J. Mazza-Stalder, P. Bart, T. Roger, T. Calandra, L. Nicod, and A. Harari. 2013. Lack of
479 *Mycobacterium tuberculosis*-specific interleukin-17A-producing $CD4^+$ T cells in active
480 disease. *Eur J Immunol* 43(3):939-948. doi: 10.1002/eji.201243090.
481 20. Ogongo, P., L. B. Tezera, A. Ardain, S. Nhamoyebonde, D. Ramsuran, A. Singh, A.
482 Ng'oepe, F. Karim, T. Naidoo, K. Khan, K. J. Dullabh, M. Fehlings, B. H. Lee, A. Nardin,
483 C. S. L. Arlehamn, A. Sette, S. M. Behar, A. J. C. Steyn, R. Madansein, H. N. Kløverpris,
484 P. T. Elkington, and A. Leslie. 2021. Tissue-resident-like $CD4^+$ T cells secreting IL-17
485 control *Mycobacterium tuberculosis* in the human lung. *J Clin Invest* 131(10):e142014.
486 doi: 10.1172/JCI142014.
487 21. Nathan, A., J. I. Beynor, Y. Baglaenko, S. Suliman, K. Ishigaki, S. Asgari, C. Huang, Y.
488 Luo, Z. Zhang, K. Lopez, C. S. L. Arlehamn, J. D. Ernst, J. Jimenez, R. I. Calderón, L.
489 Lecca, I. Van Rhijn, D. B. Moody, M. B. Murray, and S. Raychaudhuri. 2021.
490 Multimodally profiling memory T cells from a tuberculosis cohort identifies cell state
491 associations with demographics, environment and disease. *Nat Immunol* 22(6):781-793.
492 doi: 10.1038/s41590-021-00933-1.
493 22. Sun, M., J. M. Phan, N. S. Kieswetter, H. Huang, K. K. Q. Yu, M. T. Smith, Y. E. Liu, C.
494 Wang, S. Gupta, G. Obermoser, H. T. Maecker, A. Krishnan, S. Suresh, N. Gupta, M.

495 Rieck, P. Acs, M. Ghanizada, S. Chiou, P. Khatri, W. H. Boom, T. R. Hawn, C. M. Stein,
496 H. Mayanja-Kizza, M. M. Davis, and C. Seshadri. 2024. Specific CD4$^+$ T cell phenotypes
497 associate with bacterial control in people who 'resist' infection with *Mycobacterium*
498 *tuberculosis*. *Nat Immunol* 25(8):1411-1421. doi: 10.1038/s41590-024-01897-8.
499 23. Khader, S. A., G. K. Bell, J.E. Pearl, J. J. Fountain, J. Rangel-Moreno, G. E. Cilley, F.
500 Shen, S. M. Eaten, S. L. Gaffen, S. L. Swain, R. M. Locksley, L. Haynes, T. D. Randall,
501 and A. M. Cooper. 2007. IL-23 and IL-17 in the establishment of protection pulmonary
502 CD4$^+$ T cell responses after vaccination and during *Mycobacterium tuberculosis*
503 challenge. Nat Immunol 8(4):369-377. doi: 10.1038/ni1449.
504 24. Gopal, R., L. Monin, S. Slight, U. Uche, E. Blanchard, B. A. F. Junecko, R. Ramos-
505 Payan, C. L. Stallings, T. A. Reinhart, J. K. Kolls, D. Kaushal, U. Nagarajan, J. Rangel-
506 Moreno, and S. A. Khader. 2014. Unexpected Role for IL-17 in Protective Immunity
507 against Hypervirulent *Mycobacterium tuberculosis* HN878 Infection. *PLoS Pathog*
508 10(5):e1004099. doi: 10.1371/journal.ppat.1004099.
509 25. Segueni, N., E. Tritto, M. Bourigault, S. Rose, F. Erard, M. L. Bert, M. Jacobs, F. D.
510 Padova, D. P. Stiehl, P. Moulin, D. Brees, S. Chibout, B. Ryffel, M. Kammüller, and V. F.
511 Quesniaux. 2016. Controlled *Mycobacterium tuberculosis* infection in mice under
512 treatment with anti-IL-17A or IL-17F antibodies, in contrast to TNFα neutralization. *Sci*
513 *Rep* 6:36923. doi: 10.1038/srep36923.
514 26. Aguilo, N., S. Alvarez-Arguedas, S. Uranga, D. Marinova, M. Monzón, J. Badiola, and C.
515 Martin. 2016. Pulmonary but Not Subcutaneous Delivery of BCG Vaccine Confers
516 Protection to Tuberculosis-Susceptible Mice by an Interleukin 17-Dependent
517 Mechanism. *J Infect Dis* 213(5):831-839. doi: 10.1093/infdis/jiv503.
518 27. Jong, R. M., E. Van Dis, S. B. Berry, X. Nguyenla, A. Baltodano, G. Pastenkos, C. Xu, D.
519 Fox, N. Yosef, S. M. McWhirter, and S. A. Stanley. 2022. Mucosal Vaccination with Cyclic
520 Dinucleotide Adjuvants Induces Effective T Cell Homing and IL-17-Dependent Protection

521 against *Mycobacterium tuberculosis* Infection. *J Immunol* 208(2):407-419. doi:
522 10.4049/jimmunol.2100029.
523 28. Stanley, S. A., S. Raghavan, W. W. Hwang, and J. S. Cox. 2003. Acute infection and
524 macrophage subversion by *Mycobacterium tuberculosis* require a specialized secretion
525 system. *PNAS* 100(22):13001-13006. doi: 10.1073/pnas.2235593100.
526 29. Stanley, S. A., J. E. Johndrow, P. Manzanillo, and J. S. Cox. 2007. The Type I IFN
527 Response to Infection with *Mycobacterium tuberculosis* Requires ESX-1-Mediated
528 Secretion and Contributes to Pathogenesis. *J Immunol* 178(5):3143-3152. doi:
529 10.4049/jimmunol.178.5.3143.
530 30. Simeone, R., A. Bobard, J. Lippmann, W. Bitter, L. Majlessi, R. Brosch, and J. Enninga.
531 2012. Phagosomal Rupture by *Mycobacterium tuberculosis* Results in Toxicity and Host
532 Cell Death. *PLoS Pathog* 8(2):e1002507. doi: 10.1371/journal.ppat.1002507.
533 31. Romagnoli, A., M. P. Etna, E. Giacomini, M. Pardini, M. E. Remoli, M. Corazzari, L.
534 Falasca, D. Goletti, V. Gafa, R. Simeone, G. Delogu, M. Piacentini, R. Brosch, G. M.
535 Fimia, and E. M. Coccia. 2012. ESX-1 dependent impairment of autophagic flux by
536 *Mycobacterium tuberculosis* in human dendritic cells. *Autophagy* 8(9):1357-1370. doi:
537 10.4161/auto.20881.
538 32. Cox, J. S., B. Chen, M. McNeil, and W. R. Jacobs Jr. 1999. Complex lipid determines
539 tissue-specific replication of *Mycobacterium tuberculosis* in mice. *Nature* 402(6757):79-
540 83. doi: 10.1038/47042.
541 33. Barczak, A. K., R. Avraham, S. Singh, S. S. Luo, W. R. Zhang, M. Bray, A. E. Hinman, M.
542 Thompsan, R. M. Nietupski, A. Golas, P. Montgomery, M. Fitzgerald, R. S. Smith, D. W.
543 White, A. D. Tischler, A. E. Carpenter, and D. T. Hung. 2017. Systemic, multiparametric
544 analysis of *Mycobacterium tuberculosis* intracellular infection offers insight into
545 coordinated virulence. *PLoS Pathog* 13(5):e1006363. doi:
546 10.1371/journal.ppat.1006363.

547 34. Schlitzer, A., N. McGovern, P. Teo, T. Zelante, K. Atarashi, D. Low, A. W. S. Ho, P. See,
548 A. Shin, P. S. Wasan, G. Hoeffel, B. Malleret, A. Heiseke, S. Chew, L. Jardine, H. A.
549 Purvis, C. M. U. Hilkens, J. Tam, M. Poidinger, E. R. Stanley, A. B. Krug, L. Renia, B.
550 Sivasankar, L. G. Ng, M. Collin, P. Ricciardi-Castagnoli, K. Honda, M. Haniffa, and F.
551 Ginhoux. 2013. IRF4 Transcription Factor-Dependent CD11b^{+} Dendritic Cells in Human
552 and Mouse Control Mucosal IL-17 Cytokine Responses. *Immunity* 38(5):970-983. doi:
553 10.1016/j.immuni.2013.04.011.\
554 35. Soldevilla, P., C. Vilaplana, and P. Cardona. 2022. Mouse Models for *Mycobacterium*
555 *tuberculosis* Pathogenesis: Show and Do Not Tell. *Pathogens* 12(1):49. doi:
556 10.3390/pathogens12010049.
557 36. Andersen, P., Å. B. Andersen, A. L. Sørensen, and S. Nagai. 1995. Recall of Long-Lived
558 Immunity to *Mycobacterium tuberculosis* Infection in Mice. *J Immunol* 154(7):3359-3372.
559 doi: 10.4049/jimmunol.154.7.3359.
560 37. Bekmurzayeva, A., M. Sypabekova, and D. Kanayeva. 2013. Tuberculosis diagnosis
561 using immunodominant, secreted antigens of *Mycobacterium tuberculosis*. *Tuberculosis*
562 93(4):381-388. doi: 10.1016/j.tube.2013.03.003.
563 38. Babaki, M. K. Z., S. Soleimanpour, and S. A. Rezaee. 2017. Antigen 85 complex as a
564 powerful *Mycobacterium tuberculosis* immunogene: Biology, immune-pathogenicity,
565 applications in diagnosis, and vaccine design. *Microb Pathog* 112:20-29. doi:
566 10.1016/j.micpath.2017.08.040.
567 39. Dileepan, T., J. L. Linehan, J. J. Moon, M. Pepper, M. K. Jenkins, and P. P. Cleary. 2011.
568 Robust antigen specific th17 T cell response to group A Streptococcus is dependent on
569 IL-6 and intranasal route of infection. *PLoS Pathog* 7(9):e1002252. doi:
570 10.1371/journal.ppat.1002252.
571 40. Tan, H., Sattler, M., and P. Zou. 2022. Albumin-binding as a universal strategy for half-life
572 extension. *Japan J Res* 3(1):1-5. doi: 10.3342512690-8077.1043.

573 41. Sullivan, B. M., O. Jobe, V. Lazarevic, K. Vasquez, R. Bronson, L. H. Glimcher, and I.
574 Kramnik. 2005. Increased Susceptibility of Mice Lacking T-bet to Infection with
575 *Mycobacterium tuberculosis* Correlates with Increased IL-10 and Decreased IFN-γ
576 Production. *J Immunol* 175(5):4593-4602. doi: 10.4049/jimmunol.175.7.4593.
577 42. Sallin, M. A., S. Sakai, K. D. Kauffman, H. A. Young, J. Zhu, and D. L. Barber. 2017. Th1
578 Differentiation Drives the Accumulation of Intravascular, Non-protective CD4 T Cells
579 during Tuberculosis. *Cell Rep* 18(13):3091-3104. doi: 10.1016/j.celrep.2017.03.007.
580 43. Hinman, A. E., C. Jani, S. C. Pringle, W. R. Zhang, N. Jain, A. J. Martinot, and A. K.
581 Barczak. 2021. *Mycobacterium tuberculosis* canonical virulence factors interfere with a
582 late component of the TLR2 response. *eLife* 10:e73984. doi: 10.7554/eLife.73984.
583 44. Augenstreich, J., A. Arbues, R. Simeone, E. Haanappel, A. Wegener, F. Sayes, F. Le
584 Chevalier, C. Chalut, W. Malaga, C. Guilhot, R. Brosch, and C. Astarie-Dequeker. 2017.
585 ESX-1 and phthiocerol dimycocerosates of *Mycobacterium tuberculosis* act in concert to
586 cause phagosomal rupture and host cell apoptosis. *Cell Microbiol* 19(7):e12726. doi:
587 10.1111/cmi.12726.
588 45. Crosskey, T. D., K. S. H. Beckham, and M. Wilmanns. 2020. The ATPases of the
589 mycobacterial type VII secretion system: Structural and mechanistic insights into
590 secretion. *Prog Biophys Mol Biol* 152:25-34. doi: 10.1016/j.pbiomolbio.2019.11.008.
591 46. Ji, D. X., L. H. Yamashiro, K. J. Chen, N. Mukaida, I. Kramnik, K. H. Darwin, and R. E.
592 Vance. 2019. Type I interferon-driven susceptibility to *Mycobacterium tuberculosis* is
593 mediated by IL-1Ra. *Nat Microbiol* 4(12):2128-2135. doi: 10.1038/s41564-019-0578-3.
594 47. Lai, R., T. Williams, T. Rakib, J. Lee, and S. M. Behar. 2024. Heterogeneity in lung
595 macrophage control of *Mycobacterium tuberculosis* is modulated by T cells. *Nat*
596 *Commun* 15(1):5710. doi: 10.1038/s41467-024-48515-7.
597 48. Amelio, P., D. Portevin, J. Hella, K. Reither, L. Kamwela, O. Lweno, A. Tumbo, L.
598 Geoffrey, K. Ohmiti, S. Ding, G. Pantaleo, C. Daubenberger, and M. Perreau. 2019. HIV

599 Infection Functionally Impairs *Mycobacterium tuberculosis*-Specific CD4 and CD8 T-Cell
600 Responses. *J Virol* 93(5):e01728-18. doi: 10.1128/jvi.01728-18.
601 49. Geremew, D., M. Melku, A. Endalamaw, B. Woldu, A. Fasil, M. Negash, H. W. Baynes,
602 H. Geremew, T. Teklu, T. Deressa, B. Tessema, and U. Sack. 2020. Tuberculosis and its
603 association with CD4+ T cell count among adult HIV positive patients in Ethiopian
604 settings: a systemic review and meta-analysis. *BMC Infect Dis* 20(1):325. doi:
605 10.1186/s12879-020-05040-4.
606 50. Van Dis, E., K. M. Sogi, C. S. Rae, K. E. Sivick, N. H. Surh, M. L. Leong, D. B. Kanne, K.
607 Metchette, J. J. Leong, J. R. Bruml, V. Chen, K. Heydari, N. Cadieux, T. Evans, S. M.
608 McWhirter, T. W. Dubensky Jr., D. A. Portnoy, and S. A. Stanley. 2018. STING-Activating
609 Adjuvants Elicit a Th17 Immune Response and Protect against *Mycobacterium*
610 *tuberculosis* Infection. *Cell Rep* 23(5):1435-1447. doi: 10.1016/j.celrep.2018.04.003.
611 51. Watson, R. O., S. L. Bell, D. A. MacDuff, J. M. Kimmey, E. J. Diner, J. Olivas, R. E.
612 Vance, C. L. Stallings, H. W. Virgin, and J. S. Cox. 2015. The cytosolic sensor cGAS
613 detects *Mycobacterium tuberculosis* DNA to induce type I interferons and activate
614 autophagy. *Cell Host Microbe* 17(6):811-819. doi: 10.1016/j.chom.2015.05.004.
615 52. Rojas, I. M. L., W. Mok, F. E. Pearson, Y. Minoda, T. J. Kenna, R. T. Barnard, and K. J.
616 Radford. 2017. Human Blood CD1c^{+} Dendritic Cells Promote Th1 and Th17 Effector
617 Function in Memory CD4^{+} T cells. Front Immunol 8:971. doi: 10.3389/fimmu.2017.00971.
618 53. Stadhouders, R., E. Lubberts, and R. W. Hendriks. 2018. A cellular and molecular view
619 of T helper 17 cells plasticity in autoimmunity. *J Autoimmun* 87:1-15. doi:
620 10.1016/j.jaut.2017.12.007.
621

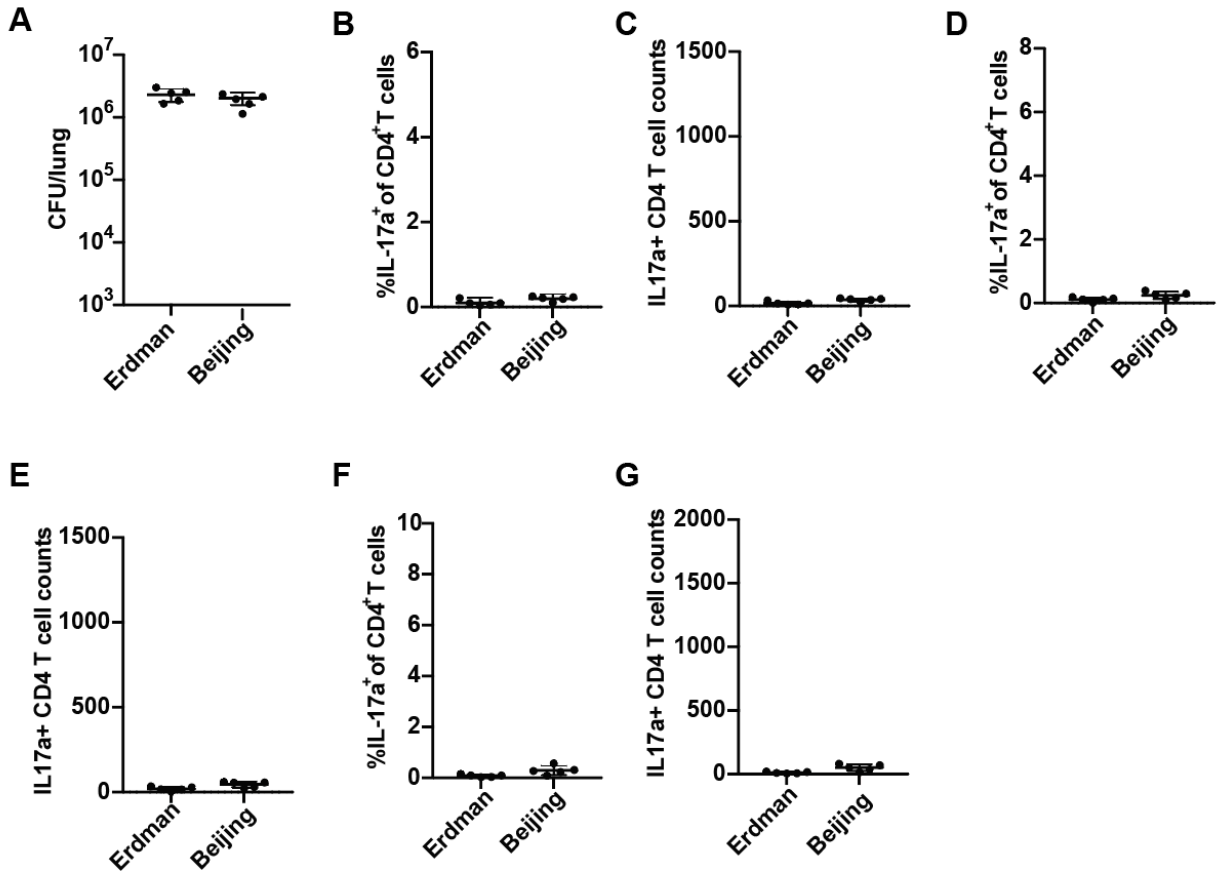

Figure S1. Mice were infected with either the Erdman or Beijing strain of Mtb via the aerosol route and evaluated at 21dpi for **(A)** CFU in the lungs or **(B-G)** IL-17a$^+$ CD4$^+$ T cells in the lungs. **(B,C)** unstimulated, **(D,E)** restimulated with Antigen 85B peptide, **(F,G)** restimulated with ESAT-6 peptide. Representative experiment of 2.

631

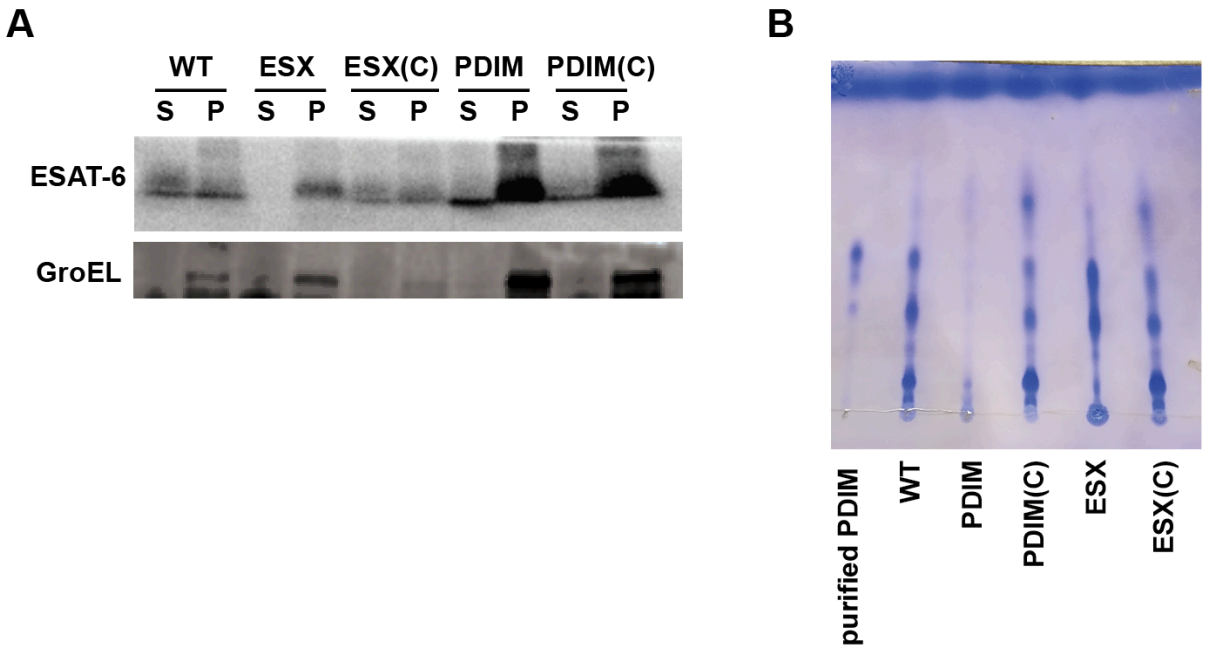

632

633 **Figure S2: Mtb Erdman PDIM mutants secrete ESAT-6 and ESX-1 mutants produce PDIM**

634 **(A)** WT, Δ*eccC1* (ESX), complemented Δ*eccC1::eccC1* (ESX(C), *fadD28::tn* (PDIM), or

635 *fadD28::tn* + p*fadD28* (PDIM(C)) *M. tuberculosis* Erdman strain were cultured in Sauton's

636 complete media without Tween-80 for 5 days. Cell lysate and culture supernatant were

637 processed through SDS-PAGE and Western blot analysis. Anti-ESAT-6 antibody was used for

638 detecting ESAT-6. Anti-GroEL antibody was used as a loading control for the supernatant

639 fraction. Results shown are from 1 experiment representative of 2 independent experiments. **(B)**

640 WT, Δ*eccC1* (ESX), complemented Δ*eccC1::eccC1* (ESX(C), *fadD28::tn* (PDIM), or *fadD28::tn* +

641 p*fadD28* (PDIM(C)) *M. tuberculosis* Erdman strain were cultured in 7H9 media. Outer leaflet of

642 mycomembrane was removed via hexanes wash, concentrated and separated on TLC plate

643 with 98:2 petroleum ether:acetone mobile phase. TLC plate was stained with 0.2% Coomassie

644 blue in 20% methanol. Results shown are from 1 experiment representative of 2 independent

645 experiments.

646

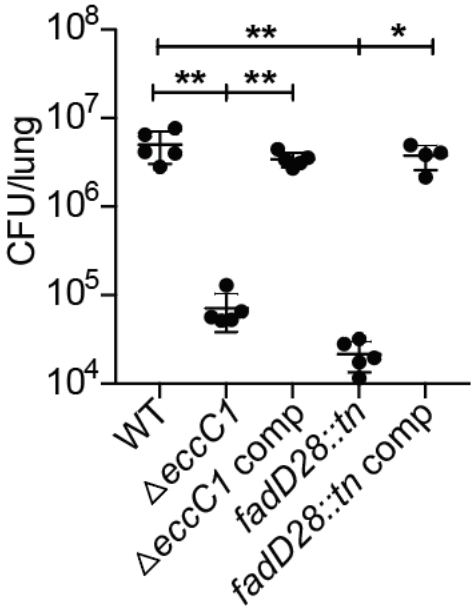

647

648

649 **Figure S3. Attenuation of ESX-1 and PDIM mutants at 21 days post infection.** WT B6 mice

650 were aerosol infected with either WT, Δ*eccC1,* Δ*eccC1::eccC1*, *fadD28::tn*, or *fadD28::tn* +

651 p*fadD28 M. tuberculosis* Erdman strain. 21 days post infection, mice were sacrificed, and CFU

652 were enumerated from lung lysates. *, $p < 0.05$; **, $p < 0.01$ (unpaired nonparametric Mann-

653 Whitney U test).

654

655

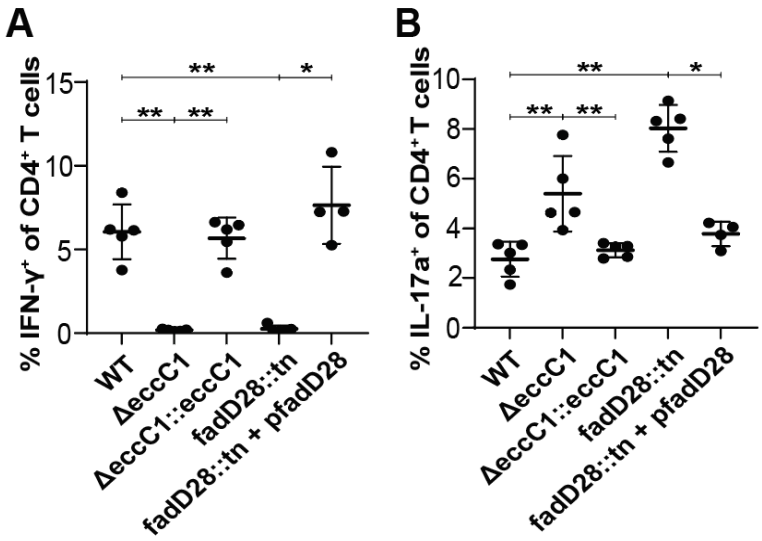

656

657 **Figure S4: Antigen 85b stim resembles ESAT-6 stimulation for IFN-γ and IL-17a staining**

658 **of CD4$^+$ T cells.** As in Figure 3, WT B6 mice were aerosol infected with either WT, Δ*eccC1,*

659 Δ*eccC1::eccC1*, *fadD28::tn*, or *fadD28::tn* + p*fadD28 M. tuberculosis* Erdman strain. 21 days

660 post infection, mice were sacrificed, lung single cell homogenates were stimulated with Antigen

661 85b peptide pool and measured for lung **(A)** IFN-γ$^+$ CD4$^+$ T cells and **(B)** IL-17a$^+$ CD4$^+$ T cells by

662 flow cytometry. Results in A and B are representative of 2 independent experiments. *, $p < 0.05$;

663 **, $p < 0.01$ (unpaired nonparametric Mann-Whitney U test

664

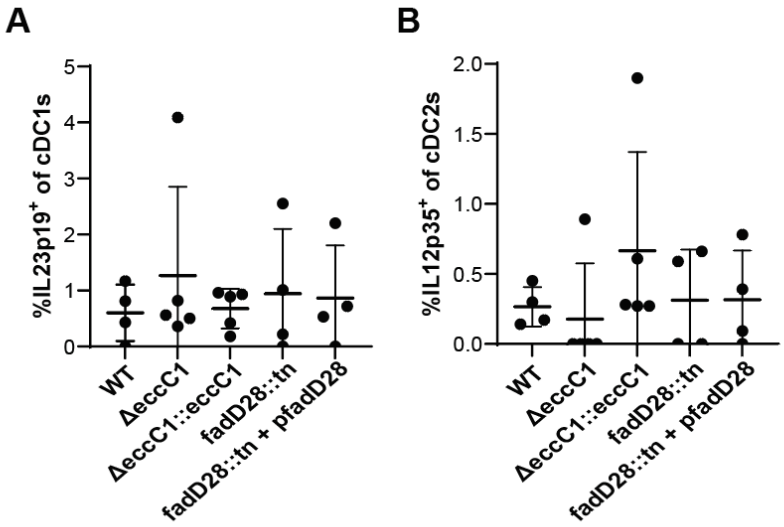

665

666 **Figure S5: There is little to no IL-23 p19 expression in cDC1s and IL-12 p35 expression in**

667 **cDC2s during Mtb infection.** As in Figure 5, WT B6 mice were aerosol infected with WT,

668 Δ*eccC1,* Δ*eccC1::eccC1*, *fadD28::tn*, or *fadD28::tn* + p*fadD28 M. tuberculosis* Erdman strain.

669 21 days post infection, mice were sacrificed, mediastinal lymph nodes were extracted, and

670 processed for ICS. Analysis of **(A)** IL-23 p19^{+} cDC1s and **(B)** IL-12 p35^{+} cDC2s by flow

671 cytometry. Results in A and B are representative of 2 independent experiments. (unpaired

672 nonparametric Mann-Whitney U test).